Fabrication and characterization of face-centered-cubic void dots photonic crystals in a solid polymer material

Guangyong Zhou, Michael James Ventura, Michael Ross Vanner, and Min Gu[a)]
Centre for Micro-Photonics & CUDOS, Faculty of Engineering and Industrial Sciences, Swinburne University of Technology, P.O. Box 218, Hawthorn, Victoria 3122, Australia

(Received 3 May 2004; accepted 2 November 2004; published online 22 December 2004)

Spherical void dots with a diameter of 1.2–1.8 μm have been generated in a solid polymer material by use of the ultrafast laser driven micro-explosion method. Micron-sized structures with a face-centered cubic lattice stacked in the [100] and [111] directions have been fabricated. Confocal microscopic images show the high uniformity of the fabricated structures. Photonic stopgaps with a suppression rate of approximately 70% as well as the second-order stopgaps have been observed in both directions. It is shown that the dependence of the stopgaps on the illumination angle in the [100] direction is significantly different from that in the [111] direction. © *2005 American Institute of Physics*. [DOI: 10.1063/1.1844039]

Photonic crystals are artificial periodic dielectric structures that can control the behavior of light in a manner analogous to the way in which semiconductor crystals control the behavior of electrons.[1,2] The unique properties of photonic crystals may result in novel devices which could find broad applications in integrated optics and all-optics communication networks. By tightly focusing ultrafast laser light into transparent solid materials, micro-explosion occurs at the focal point, where the material is ejected from the center forming a void cavity surrounded by a region of compressed material.[3–5] Smooth void dots and void channels have been generated in glass[6,7] and polymer materials[8–10] and stacked into two-dimensional and three-dimensional (3D) photonic crystals. Although the refractive index of polymer and glass is not high enough to open a complete photonic band gap, partial band gaps (stopgaps) can be achieved in the near-infrared wavelength range and could be used for superprisms where a complete band gap is not prerequisite.[11,12] The lower power threshold to generate void dots in polymers and the easy doping of some functional materials such as quantum dots and organic dyes are the advantages of the polymer materials compared with glass materials.

Void channel based woodpile structures in polymer can easily open a partial band gap and higher order gaps in the stack direction.[8,13] However, it is not easy to achieve different types of lattice structures and the gaps are not sensitive to the angle of incidence. It is more flexible to arrange void dots to fabricate arbitrary lattices.[7] A face-centered cubic (fcc) lattice is a tightly packed structure and has a square arrangement in the [100] direction and a hexagonal (triangle) arrangement in the [111] direction. One can expect different angle dependence in the two directions. In this letter, we report on the fabrication of photonic crystals with an fcc lattice and the photonic band gap properties as well as their angular dependence in different lattice directions.

The polymer material used in this work is a solidified optical adhesive (NOA 63, Norland Products Inc., USA). The experimental setup and blank sample preparation are the same as described in our previous papers[9] except that an Olympus 60×, numerical aperture (N.A.) 1.45 oil-immersion objective and a 740 nm femtosecond laser beam from a Tsunami femtosecond laser (Spectra-Physics, USA) were used in this work. The power of the laser beam and the exposure time were kept constant at 40 mW and 10 ms, respectively. The fcc structures were fabricated layer by layer parallel to the top surface of the polymer film with the top layer 5 μm below the surface.

In order to view the fabricated void dots in the fabrication (longitudinal) direction, a cuboid bulk sample was prepared and 22 rows of void dots were fabricated at different depths with a dot spacing and a row spacing of 6 and 3 μm, respectively, as illustrated in Fig. 1(a). After fabrication, the sample was rotated by 90° and viewed by use of a confocal microscope (Fluoview, Olympus, Japan). Figure 1(b) shows the reflection (left) and transmission confocal images (right) of the void dots. The strong reflection signal from the fabricated dots indicates a large refractive index change, which verifies the formation of the void.[5] Smooth and uniform void dots can be seen from the zoom-in transmission confocal

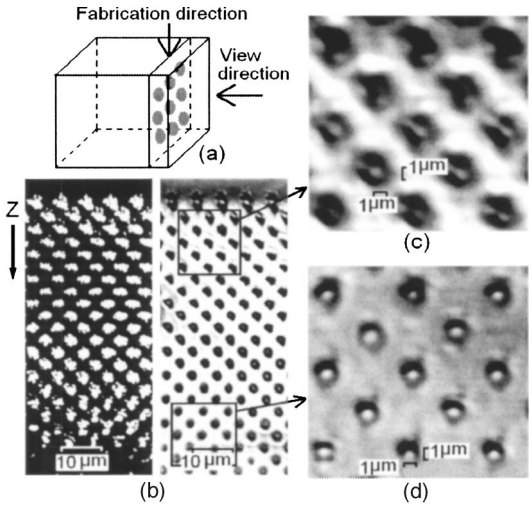

FIG. 1. Side view of the fabricated void dots in solidified NOA 63 resin by use of confocal microscopy. (a) Illustration of the void arrangement in the bulk sample; (b) reflection and transmission confocal images of the void dots at various depths; (c) and (d) zoom in images of the upper and lower parts of the transmission confocal image in (b), respectively.

[a)]Author to whom correspondence should be addressed; electronic mail: mgu@swin.edu.au

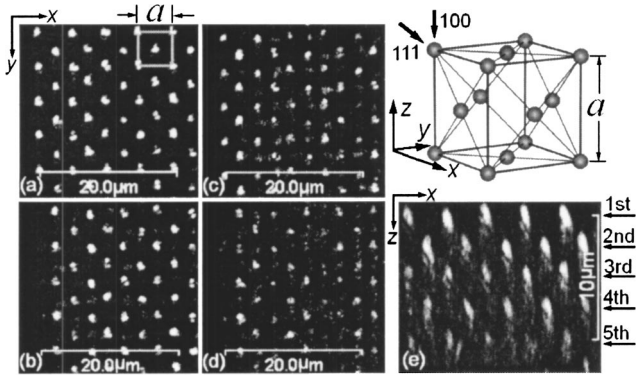

FIG. 2. Confocal reflection microscope images of the top four layers [(a)–(d)] and the *x*–*z* scanning image of the top five layers (e) of an fcc structure stacked in the [100] direction with a lattice constant of 4.96 μm. The sketch in upper-right corner shows the unit cell of the fcc lattice.

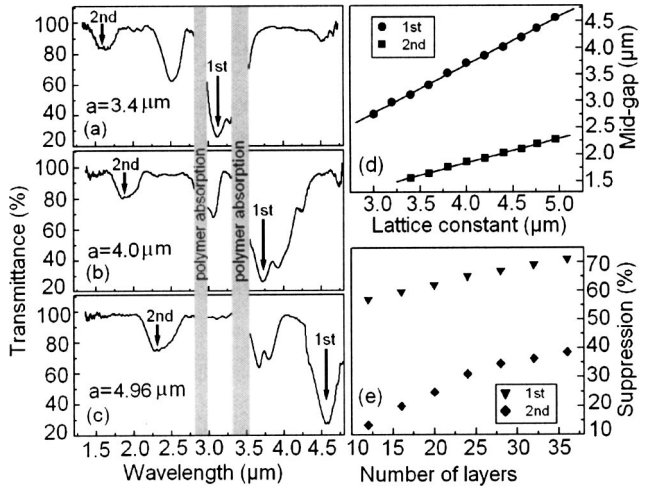

FIG. 3. Transmission spectra of 3D fcc void photonic crystals stacked in the [100] direction with different lattice constants [(a)–(c)]. The lattice constant dependence and the layer number dependence of the first- and second-order gaps are shown in (d) and (e), respectively.

images in Figs. 1(c) and 1(d). Due to the slight effect of spherical aberration caused by the refractive index mismatch between the polymer (1.56) and immersion oil (1.52),[14] the peak power at the focal point becomes lower at a deeper depth, which results in smaller voids, as shown in Figs. 1(c) and 1(d). As a result, the diameter of the dot decreases from approximately 1.8 μm near the top surface down to approximately 1.2 μm at a depth of 60 μm. It should be pointed out that the void dots are spherical which is different from the elliptical cross section of the fabricated rods in the two-photon polymerization method.[15] The possible reason is that, in the case of micro-explosion, high pressure gas exists in a void and a spherical shape is a stable state. Due to the flexibility of the polymer, voids may be reshaped to the stable spherical shape right after the formation of the void dots.

By stacking void dots layer by layer, we fabricated 3D structures with an fcc lattice in the [100] and [111] directions. The unit cell of an fcc lattice is schematically shown in Fig. 2, where the [100] and the [111] directions are indicated. In the [100] direction, parallel planes of lattice points form a periodicity of two, offset by half of a lattice constant (a) in the x or y direction. Adjacent layers are spaced by half of a. In the [111] direction, the lattice points are packed in the pattern of a hexagonal-close-packed structure with a layer periodicity of three. The light penetrates through the photonic crystals perpendicular to the polymer film in both the fabrication process and the infrared transmission spectra measurement.

Fabricated structures were examined in detail by use of confocal reflection microscopy. Figures 2(a)–2(d) show the confocal reflection images of the top four layers of voids of an fcc structure with a lattice constant of 4.96 μm stacked in the [100] direction. The scale bars generated by the microscope control program can be used as the reference because the sample was adjusted only in the z direction during the measurement. Figure 2(a) gives a clear pattern of the first layer; the unit cell is superimposed over the image, highlighting the fcc structure. Figure 2(b) shows the second layer of voids which is the same as the first layer except for shifting by half a lattice constant in the x direction. Figure 2(c) shows the voids in the third layer that is exactly the same as the first layer because the periodicity in the [100] direction is two. Consequently, the void patterns of the fourth layer and the second layer are the same, as shown in Figs. 2(b) and 2(d). Figure 2(e) shows the *x*–*z* scanning confocal reflection image of the top five layers of voids with the layer numbers marked. It can be seen that the image quality degrades along the depth, which is caused by strong scattering of upper layers.[5] As expected, the layer spacing is approximately 2.5 μm, which is equal to a half lattice constant.

Infrared transmission spectra were measured by use of a Fourier transform infrared (FTIR) spectrometer fitted with a 32×, N.A. 0.65 reflective objective (Thermo Nicolet, Madison, WI) which provides an incident hollow light cone with an outer angle of 40° and an inner angle of 15°. To reduce the range of angle of incidence, a small off-center aperture corresponding to a half angle of approximately 5° was placed in front of the FTIR objective. Illumination in the [100] and [111] directions was achieved by tilting the sample perpendicular to the resulting incidence light cone. By change of the position of the aperture and/or the gradient of the sample, different angles of incidence can be achieved.

Figures 3(a)–3(c) show the baseline-corrected transmission spectra of 28-layer fcc void dots structures stacked in the [100] direction with the lattice constant of 3.4, 4.0, and 4.96 μm, respectively. Two orders of stopgaps were observed. The suppression rate of transmission of the observed first order gap is as large as 74%. The second order stopgap located at exactly a half of the wavelength of the first order gap is also observed, with a suppression rate of approximately 20%. Both the first and second order stopgaps shift to the longer wavelengths with an increase in the lattice constant. The mid-gap wavelength dependence of the first- and the second-order stopgaps on the lattice constant are plotted in Fig. 3(d), where a linear relationship between the mid-gap wavelengths and the lattice constants can be observed. The linear fitting results show that the gradient for the second-order gap (0.46) is approximately one-half of that for the first-order gap (0.92). The dependence of photonic band gaps on the layer number for the fcc structures in the [100] direction is also studied. Figure 3(e) shows the dependence of the transmittance of the two stopgaps on the layer number for structures with a lattice constant of 4.4 μm. Increasing the layer number from 12 to 36, the suppression rate increases from 56% to 71% and from 13% to 39% for the observed first- and second-order gaps, respectively.

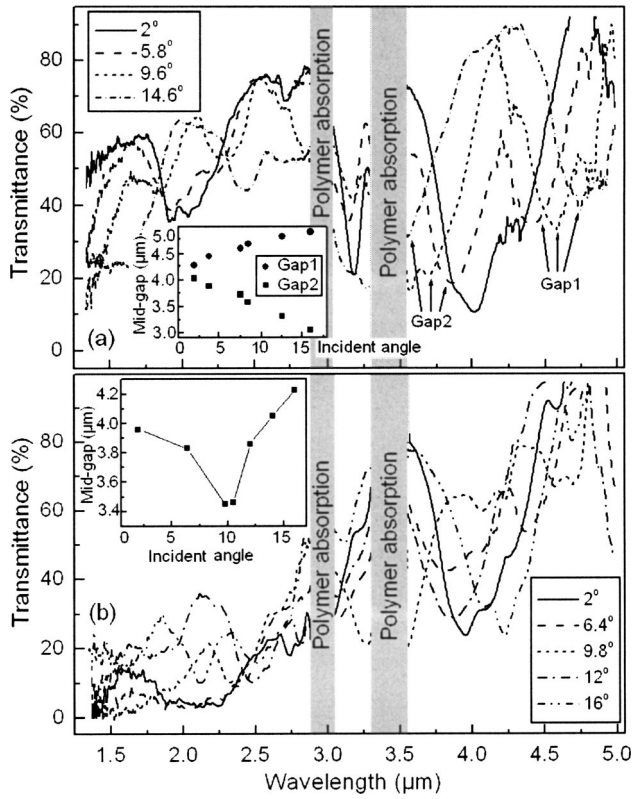

FIG. 4. Transmission spectra of 3D fcc structures stacked in the [100] direction (a) and the [111] direction (b) at different angles of incidence. The corresponding angular dependence of the photonic stopgaps are shown in the insets.

The photonic band gap properties of a photonic crystal depend on the lattice direction. Therefore the angular dependence of the band gap properties of fcc structures stacked in the [100] and the [111] directions was investigated. Figure 4(a) shows the transmission spectra of an fcc structure stacked in the [100] direction with a lattice constant of 4.44 μm at different angles of incidence. The observed first-order stopgap splits into two peaks and shifts to the opposite direction as the angle of incidence increases. The inset shows the angular dependence of the two peaks. At the angle of incidence of 16.5°, the wavelength difference between the two peaks is 1.8 μm. Figure 4(b) shows the transmission spectra of an fcc structure stacked in the [111] direction with a lattice constant of 4.9 μm at different angles of incidence. At an angle of incidence of 2° (solid curve), the first gap locates at 4 μm with a suppression rate of up to approximately 70%. The solid curve also indicates the existence of a second-order stopgap at 2 μm which locates at half of the wavelength of the observed first-order stopgap (4 μm). Increasing the angle of incidence, the behavior of the first-order gap in the [111] direction is quite different from that in the [100] direction. From Fig. 4(b), one can see that the first-order stopgap shifts to shorter wavelength as the angle of incidence increase up to approximately 10°, and then shifts to longer wavelength as the angle of incidence further increases. The dependence of the first-order stopgap on the angle of incidence is shown in the inset of Fig. 4(b). The different angle dependence properties in the [100] and the [111] directions may be caused by the different void dot arrangement in the two directions. For an fcc lattice, there is a square arrangement in the [100] direction and a hexagonal (triangle) arrangement in the [111] direction.

In summary, 3D fcc photonic crystals stacked in the [100] and [111] directions were fabricated by generating spherical void dots in solidified NOA 63 resin, which are verified by use of confocal reflection and transmission microscopy. Photonic stopgaps including the second-order stopgaps were observed for the fcc structures stacked in both the [100] and [111] directions. The photonic stopgap in both these directions are sensitive to the angle of incidence and show different angular dependence properties. Such a sensitive angular dependence of the band gap structure may prove advantageous in angle-depedent photonic devices such as superprisms.[11,12]

This work was produced with the assistance of the Australian Research Council under the ARC Centres of Excellence Program. CUDOS (the Centre for Ultrahigh-bandwidth Devices for Optical Systems) is an ARC Centre of Excellence.

[1]E. Yablonovitch, Phys. Rev. Lett. **58**, 2059 (1987).
[2]S. John, Phys. Rev. Lett. **58**, 2486 (1987).
[3]E. N. Glezer and E. Mazur, Appl. Phys. Lett. **71**, 882 (1997).
[4]K. Yamasaki, S. Juodkazis, M. Watanabe, H.-B. Sun, S. Matsuo, and H. Misawa, Appl. Phys. Lett. **76**, 1000 (2000).
[5]D. Day and M. Gu, Appl. Phys. Lett. **80**, 2404 (2002).
[6]H.-B. Sun, Y. Xu, S. Matsuo, and H. Misawa, Opt. Rev. **6**, 396 (1999).
[7]H.-B. Sun, Y. Xu, S. Juodkazis, K. Sun, M. Watanabe, S. Matsuo, H. Misawa, and J. Nishii, Opt. Lett. **26**, 325 (2001).
[8]H.-B. Sun, Y. Xu, K. Sun, S. Juodkazis, M. Watanabe, S. Matsuo, H. Misawa, and J. Nishii, Mater. Res. Soc. Symp. Proc. **605**, 85 (2000).
[9]M. J. Ventura, M. Straub, and M. Gu, Appl. Phys. Lett. **82**, 1649 (2003).
[10]G. Zhou M. J. Ventura, M. Straub, M. Gu, A. Ono, S. Kawata, X. H. Wang, and Y. Kivshar, Appl. Phys. Lett. **84**, 4415 (2004).
[11]S. Lin, V. M. Hietala, L. Wang, and E. D. Jones, Opt. Lett. **21**, 1771 (1996).
[12]T. Baba and M. Nakamura, IEEE J. Quantum Electron. **38**, 909 (2002).
[13]M. Straub, M. Ventura, and M. Gu, Phys. Rev. Lett. **91**, 043901 (2003).
[14]D. Day and M. Gu, Appl. Opt. **37**, 6299 (1998).
[15]M. Straub and M. Gu, Opt. Lett. **27**, 1824 (2002).